

Force Chains, Microelasticity and Macroelasticity

C. Goldenberg^{1,*} and I. Goldhirsch^{2,†}

¹*School of Physics and Astronomy, Tel-Aviv University, Ramat-Aviv, Tel-Aviv 69978, Israel*

²*Fluid Mechanics and Heat Transfer, Tel-Aviv University, Ramat-Aviv, Tel-Aviv 69978, Israel*

(Dated: April 26, 2024)

Some recent experiments and theories suggest that (near) static granular and nanoscale materials exhibit departures from elastic behavior even at infinitesimal loadings. It is demonstrated, through a study of the forces and stress fields in finite discrete systems, that (at least some of) the pertinent phenomena are consistent with elasticity, the apparent non-elastic behavior being a manifestation of finite size, small (including sub-particle) scale effects, and small scale anisotropy. Other findings can be attributed to large scale anisotropy, disorder, and boundary conditions.

PACS numbers: 45.70.Cc, 46.25.Cc, 83.80.Fg, 61.46.+w

There are at least two classes of systems whose apparent departure from elastic mechanical response to infinitesimal perturbations has been recently discussed in the literature: granular [1] and nanoscale [2] materials. Though the former typically comprise macroscopic grains and the latter are very small solid systems, they do share at least one common property: both are typically composed of a relatively small number of constituents. While the discussion below should be relevant to both of the above classes, it employs a “granular terminology” and focuses on the latter type of materials.

A physical picture whereby forces in (near) static granular materials “propagate” (corresponding to hyperbolic PDE’s) has been suggested [3, 4]. This is in marked contrast with the elliptic, non-propagating nature of the classical equations of (static) elasticity, and seems to disqualify elastic theory as a good description for the mechanical properties of static granular matter (elasto-plastic models are commonly used by engineers in this field [5, 6]).

One of the goals of this Letter is to show that there is no contradiction between the “elastic” and “propagating” pictures. Another goal is to show how a proper understanding of the range of validity of elasticity as a coarse grained mechanical description, which is endowed with a finite (and controllable) spatial resolution, helps explain the results of some recent experiments [7, 8]. A key element in the present study is the (almost trivial) observation that small particulate systems exhibit deviations from continuum elasticity. Elastic behavior is recovered for sufficiently large systems (see below).

Consider, for instance, a particulate system subject to a point force at a boundary. As a system composed of discrete constituents cannot be isotropic on the particle scale, there should be locally preferred directions on this scale, even when the system is macroscopically isotropic. One therefore may expect the existence of “force chains” indicating a stronger transfer of the applied force along certain directions. Still, when the interparticle forces are derived from potentials (and can be linearized), the linearized forces satisfy a (discrete) elliptic set of equations, the notion of force propagation being an *approximation*

pertaining to the “strong” forces alone. Continuum theory cannot be expected to describe these microscopic interparticle *forces*. The macroscopic field which is related to the microscopic forces (in a specific way, see below) is the *stress*. Even at small, but finite, spatial resolution, the calculation of the stress tensor inherently involves averaging over the forces acting on the particles. The resulting macroscopic stress may bear little or no resemblance to the force distribution on the microscopic (particle) scale. Similarly, disorder can have a large effect at small scales, yet allow for large scale homogeneous (and possibly isotropic) elasticity.

The discussion below is limited to linear elasticity. Therefore it is sufficient to consider harmonic interactions of the constituents. Although non-cohesive grains cannot attract each other, this choice of model can be justified a-priori by noting that in experimental situations gravity (and/or confining forces) ensure that all forces are compressional (else the system rearranges) and a-posteriori by checking the solutions of the model. Notice that when the effects of gravity are subtracted (as in some studies [7, 8]) the residual intergrain effective interaction can be attractive. As should become evident below, the validity of the conclusions transcends that of the employed models. Furthermore, the results described below are not limited to systems with specific values of the mean coordination number (e.g., “isostatic” systems). Frictional effects (hence, piles) are not considered here.

Consider, as in an experiment described in [7], a two dimensional (2D) slab, composed of uniform disks (of diameter d) whose centers are positioned on a triangular lattice, as depicted in Fig. 1. The slab is attached to a rigid floor. Nearest neighbors are assumed to be coupled by uniform linear springs (of rest length d). As in the experiment, a downward force is applied to a disk in the top row. The interparticle force are depicted in Fig. 1. One can identify “force chains” through which the “strong” forces are transmitted. The corresponding experimental forces have been studied by optical means, through which the *internal* particle stresses were measured. As the latter are concentrated near particle con-

tacts, they indeed provide a measure of the interparticle forces. Fig. 2 shows the calculated force distribution at different depths. Figs. 1,2 closely correspond to the experimental findings. However, microelastic measurements do not directly reveal the bulk stress field. Fig. 3 depicts the normal vertical stress component, σ_{zz} , as calculated using the following exact formula [9]:

$$\sigma_{\alpha\beta}(\mathbf{r}, t) = \frac{1}{2} \sum_{i=1}^N \sum_{j \neq i}^N f_{i/j\alpha} r_{ij\beta} \int_0^1 ds \phi(\mathbf{r} - \mathbf{r}_i(t) + s\mathbf{r}_{ij}(t)),$$

where $\mathbf{r}_i(t)$ is the center of particle i , $\mathbf{r}_{ij}(t) \equiv \mathbf{r}_i(t) - \mathbf{r}_j(t)$, and $\mathbf{f}_{i/j}$ is the force exerted on particle i by particle j . Greek indices denote Cartesian components. The coarse graining function [9] is $\phi(\mathbf{r}) = \frac{1}{\pi w^2} e^{-(|\mathbf{r}|/w)^2}$, with $w = d$, which provides a rather fine resolution. The force chains are not evident any more. The model considered here can be shown [10] to correspond in the continuum limit to an isotropic 2D elastic medium. Therefore one can compare the stress obtained from the microscopic force distribution with that of the corresponding elastic solution.

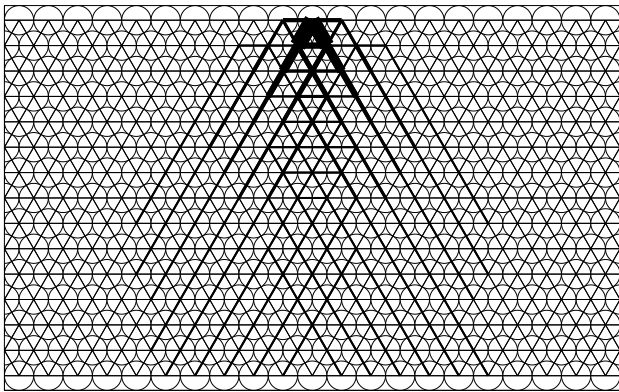


FIG. 1: Force chains in a 2D triangular lattice. A vertical force is applied to the center particle in the top layer. The line widths are proportional to the forces. Only the central region of the lattice is shown (the entire lattice comprises 15 layers of 41 particles each).

Fig. 4 presents a comparison between the vertical stress exerted on the floor of the system and continuum elastic solutions. The convergence to the appropriate (rough rigid support) elastic stress distribution for a sufficient number of layers is evident. A theory which includes the lowest order corrections to continuum elasticity [10] fits the discrete data for much smaller numbers of layers.

Consider next an anisotropic medium, obtained by taking the spring constants K_1 in the horizontal direction to be different from those of the oblique springs, K_2 . As shown in Fig. 5, the obtained force distribution (on the floor) is either single peaked (narrower than the isotropic one for $K_2/K_1 < 1$, wider for $K_2/K_1 > 1$) or double peaked for sufficiently large K_2/K_1 . The double peaked distribution is similar to that obtained from hyperbolic

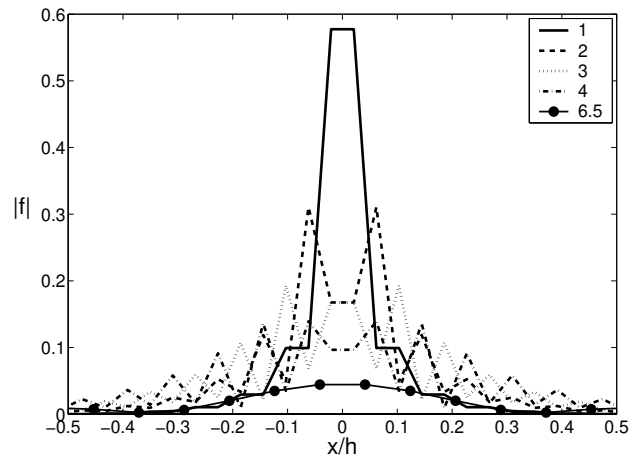


FIG. 2: The norms of the interparticle forces, $|\mathbf{f}|$, at several depths in the triangular lattice, vs. the horizontal position, x , normalized by the slab height, h . A unit force is applied on the top layer at $x = 0$. The depths are in layer numbers.

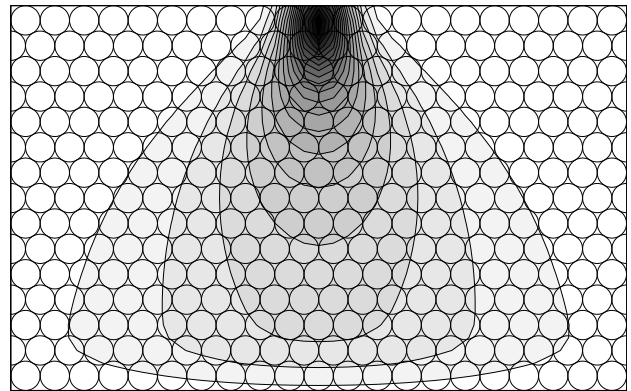


FIG. 3: Contour plot of the vertical stress component, σ_{zz} , in the 2D triangular lattice, in the same region shown in Fig. 1.

models. Indeed, for very large K_2/K_1 , the force under the point of application decreases to zero. This indicates that phenomena similar to those suggested by the hyperbolic models can be obtained using *anisotropic* elasticity. The equations of anisotropic elasticity, which are of course elliptic, can approach hyperbolicity in the limit of very large anisotropy (see also [3]).

The effect of disorder on the force chains, observed in [7], can be qualitatively reproduced in a perturbed triangular lattice. Fig. 6 depicts the force chains for such a perturbed lattice, where a random number, uniformly distributed in the range $[-\frac{d}{4}, \frac{d}{4}]$, is added to the x and y coordinates of the particles, except those of the fixed bottom row. Only particles whose centers are less than $c_{\max} = 1.15d$ apart are connected by springs. The main difference with respect to the case of a regular lattice is the fact that here the force chains are somewhat shorter. This effect is less pronounced for a higher connectivity, obtained by taking $c_{\max} = 1.3d$ (yielding a connectivity

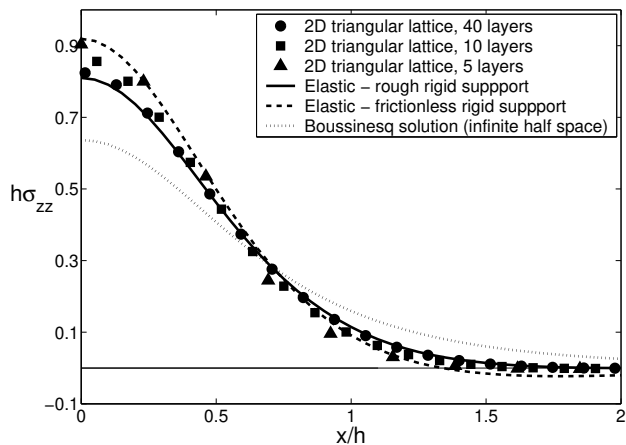


FIG. 4: The vertical stress on the bottom of the 2D triangular lattice, compared to continuum elastic solutions. The results are scaled by h . Note: $\sigma_{zz}\left(\frac{x}{h}\right) = \sigma_{zz}\left(-\frac{x}{h}\right)$.

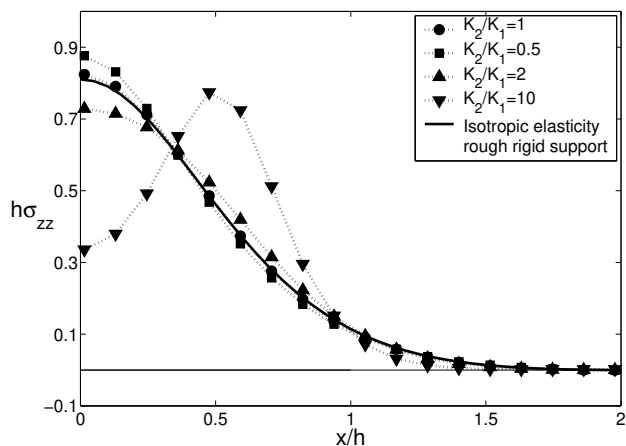


FIG. 5: The vertical stress on the bottom of an anisotropic 2D triangular lattice composed of 40 layers, compared to the isotropic elastic solution. Note: $\sigma_{zz}\left(\frac{x}{h}\right) = \sigma_{zz}\left(-\frac{x}{h}\right)$.

close to that of the regular lattice). The macroscopic stress field measured at the floor of the system for the perturbed lattices is quite close to that of the regular lattice, except for (expected) fluctuations (Fig. 7).

Very similar results to those presented above are obtained for a three dimensional (3D) system: consider a collection of particles positioned on a simple cubic lattice. As shown in [11], this system corresponds, on large scales, to an isotropic elastic continuum when the spring constants for springs coupling nearest neighbors (K_1) equal those coupling next nearest neighbors (K_2). While this model does not directly describe the interaction of granular particles, we believe it is useful for the description of the crossover between microelasticity and macroelasticity. Furthermore, as shown below, the stresses computed for this model are in close correspondence with the experimental results reported in [8]. Consider a 3D slab

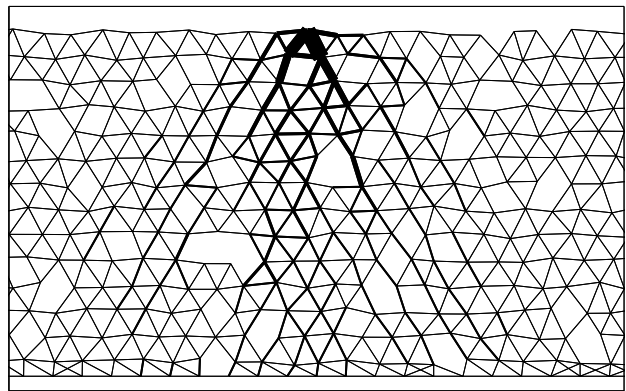


FIG. 6: Force chains in a perturbed 2D triangular lattice (15 layers), with $c_{\max} = 1.15d$ (see text).

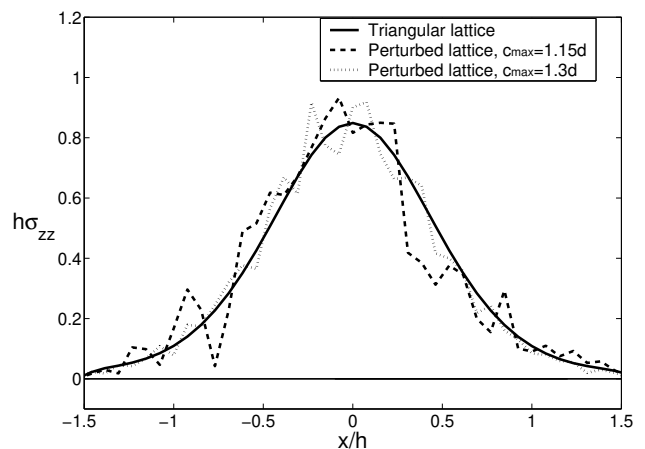


FIG. 7: The vertical stress on the bottom of a (15 layers) triangular lattice and two perturbed lattices.

of finite height, with a downward force acting on a particle in the top layer. Fig. 8 depicts the vertical stress distribution exerted on the floor for three different slab depths. A comparison with the corresponding finite slab elastic solution (for a rough or frictionless support) and the half space Boussinesq solution demonstrates that the results for discrete lattices converge to the appropriate finite slab elastic solution with increasing depth, as in the 2D case described above. The effect of small scale anisotropy (in this case, the cubic symmetry) is seen in Fig. 9, which depicts contour plots of the distribution of the vertical force on the floor. When the depth of the system is small, one can observe the effect of the underlying cubic symmetry. As this symmetry is washed out in the continuum limit, the stress crosses over to that corresponding to isotropic elasticity.

It is interesting to note that the results obtained for a shallow discrete slab seem to be similar to those obtained experimentally for a loose granular packing [8], for which the force distribution is narrower than that predicted by the continuum elastic solution. Since the

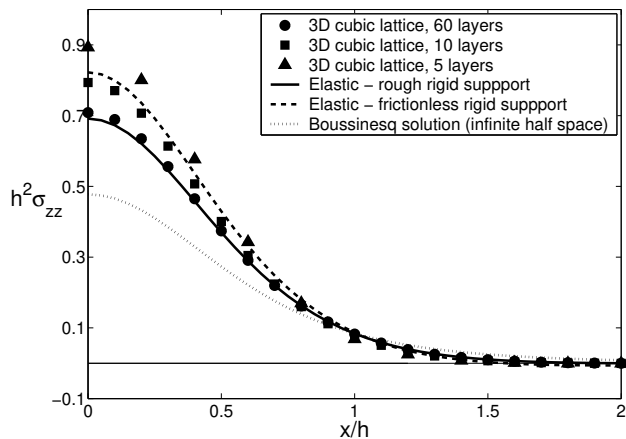


FIG. 8: The vertical stress along the x -axis on the bottom of a cubic lattice, compared to continuum elastic solutions. The results are scaled by h . Note: $h^2 \sigma_{zz} \left(\frac{x}{h} \right) = h^2 \sigma_{zz} \left(-\frac{x}{h} \right)$.

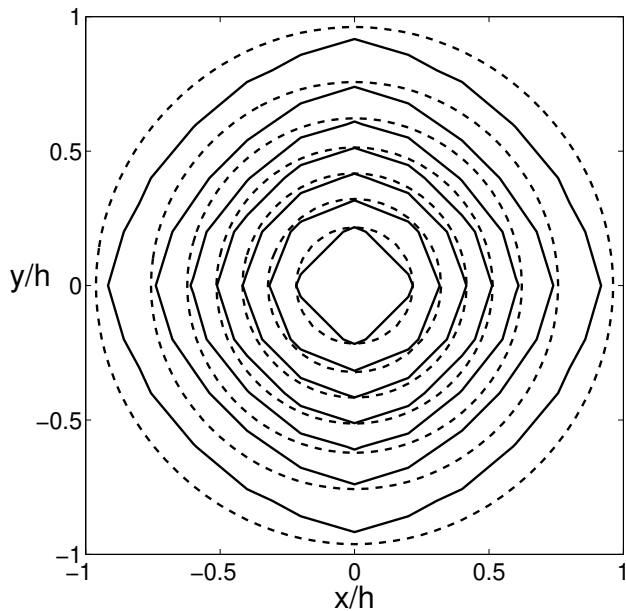


FIG. 9: A contour plot of the force distribution on the bottom of 3D slabs composed of 5 (solid contours) and 20 (dashed contours) discrete layers. The cubic anisotropy is evident for 5 layers, while the distribution appears isotropic for 20 layers.

experimental system is disordered, this similarity may be accidental. In contrast, for a dense packing, experiments show a wider distribution. As mentioned in [8] and above, this can be explained by anisotropic effects (e.g., in the discrete model considered here, increasing K_2 with respect to K_1 results in a wider distribution). Also recall that the results presented above for an anisotropic 2D system show that anisotropy can yield both narrower and wider distributions. The method of preparation of the experimental system [8] suggests that it may be bet-

ter modeled by a number of isotropic elastic layers of variable elastic moduli. Calculations show that the resulting force distribution on the floor can be wider or narrower than the solution for a homogeneous slab, depending on the distribution of elastic constants of the layers [6, 10]. In addition, the rigidity of the supporting floor is consequential [6, 10]: the force distribution becomes wider the smaller the rigidity of the support.

In conclusion, evidence in favor of a (continuum) elastic description of discrete particle systems is presented. While not discussed here, the notion of macroscopic strain (expressed in terms of the microscopic displacements) can be shown to be as relevant for small elastic systems as for large ones. Effects of discreteness and disorder are strong when the system is small or the resolution of the coarse grained description is fine. Force chains reflect local anisotropy which is washed out in the limit of large systems or coarse resolutions. Continuum elasticity is relevant even to relatively small systems, an improved description being provided by a set of equations which take the discreteness into account but are still of elliptic nature. The experimentally observed results can be attributed to the crossover from small scale effects to the continuum, the finite depth of the slab, the degree of disorder and anisotropy (on both small and large scales), and the rigidity of the support. The above results are claimed to be equally relevant to unstressed and pre-stressed systems.

Support from the Israel Science Foundation, grant no. 39/98, is gratefully acknowledged.

* Electronic address: chayg@post.tau.ac.il

† Electronic address: isaac@eng.tau.ac.il

- [1] Focus Issue on Granular Materials, *Chaos* **9** (1999).
- [2] e.g., J.-P. Salvetat et al., *Appl. Phys. A* **69**, 255 (1999).
- [3] M. E. Cates, J. P. Wittmer, J.-P. Bouchaud and P. Claudin, *Chaos* **9**, 511 (1999) and refs. therein.
- [4] S. N. Coppersmith et al., *Phys. Rev. E* **53**, 4673 (1996); F. Radjai, S. Roux and J. J. Moreau, *Chaos* **9**, 544 (1999); J.-P. Bouchaud, P. Claudin, D. Levine and M. Otto, *Eur. Phys. J. E* **4**, 451 (2001).
- [5] R. M. Nedderman, *Statics and Kinematics of Granular Materials* (Cambridge University Press, 1992).
- [6] S. B. Savage, in *Powders and Grains 97*, 185, Ed. R. P. Behringer and J. T. Jenkins (Balkema, 1997).
- [7] J. Geng et al, *Phys. Rev. Lett.* **87**, 035506 (2000).
- [8] G. Reydellet and E. Clément, *Phys. Rev. Lett.* **86**, 3308 (2001); D. Serero et al., *cond-mat/0107626*.
- [9] B. J. Glasser and I. Goldhirsch, *Phys. Fluids* **13**, 407 (2001).
- [10] C. Goldenberg and I. Goldhirsch, unpublished.
- [11] C. Kittel, *Introduction to Solid State Physics* (Wiley, 1956).